HEALTH MONITORING OF AIRCRAFT FUSELAGE STRUCTURES USING ULTRASONIC WAVES

Z. Q. Zhou*, W. K. Chiu*, M. K. Bannister**
***Department of Mechanical Engineering, Monash University, PO Box 31, Clayton, VIC, 3800, Australia**
****Cooperative Research Centre for Advanced Composite Structures, 506 Lorimer Street, Fishermans Bend, VIC, 3207, Australia**

Abstract

A series of numerical and experimental investigations were conducted into the use of acousto-ultrasonic stress waves for the detection of defects in a typical aluminium (Al) aircraft fuselage structure. This structure consists of a skin, stringer and frame. PZT actuator/sensor pairs placed on the stringer were able to detect stringer cracks but not frame cracks. Actuators on the stringer and sensors on the frame were able to detect both stringer and frame cracks however the signal intensity was very low.

1 Introduction

Structural Health Monitoring (SHM) is becoming increasingly important not only for preventing catastrophic failures but also for the uninterrupted operation and prolonged service life of high-value engineering structures. Aerospace structures are usually inspected using traditional nondestructive techniques such as visual inspection, ultrasonics, radiography and eddy current. Often these traditional inspection techniques require the aircraft to be taken out of service for inspection. These inspection techniques can also be difficult to conduct in hard-to-reach areas of the aircraft. The need for increased availability of aircraft, the need for life-extension, and the demands of high performance aircraft bring about the issue of in-situ structural health monitoring. These techniques can be used to provide for continuous or in-situ structural monitoring for the aircraft.

Propagating lamb waves (or stress waves) have been shown to be sensitive to the presence of structural defects including cracks. Chimenti and Martin [1] and Cheng and Berthelot [2] have studied the application of Lamb waves to detect defects in composite plates. Bork and Challis [3], Rokhlin [4] and Todd and Challis [5] have investigated the propagation of Lamb waves through bonded joints. Rokhlin [4] studied the interaction of different Lamb modes with disbonds in adhesive joints in which plates of equal thickness are joined by a layer of adhesive. Rokhlin and Bendec [6] investigated the transmission of Lamb waves through a welded joint connecting two elastic layers. The transmission coefficient was used as for estimating the dimension of the contact region, which is an important parameter for evaluating the strength of a welded joint.

The brief review above shows a sample of work where propagating stress waves can be used for structural health monitoring. These stress waves can be generated using low-profile piezoceramic (PZT) elements. Rajic et al [7], Koh et al [8] and Koh et al [9] demonstrated how these waves can be generated using these devices. This paper examines the potential for propagating stress waves to be used to identify flaws in a structure built up from multiple elements.

2 Numerical model

2.1 General Description

In this study, a finite element model was constructed to simulate a typical aircraft

fuselage shell structure. This structure consists of a skin stiffened by stringers in the longitudinal direction and frames in the circumferential direction. The stringers were bonded to the skin and the frames were sitting on the top of the stringer. A clip was used to join the skin, the stringer and frame together by riveting. A typical arrangement of the fuselage skin with stringers, frames and clips is shown in Figure 1.

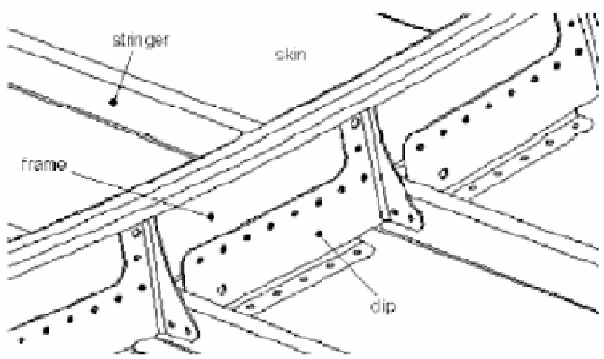

Fig. 1. Typical fuselage structure

To address the objectives of this investigation, the following analyses were conducted:

(a) a PZT actuator was located on the stringer and a PZT sensor was located further along the length of the stringer. In each of these simulations the cracks were assumed to be located between the actuator and the sensing PZT elements.

(b) a PZT actuator was located on the stringer and a PZT sensor was located on the frame of the structure.

Whilst analysis (a) was used to ascertain the sensitivity of the actuator-sensor pair with respect to their physical separation, analysis (b) was used to determine if the acousto-ultrasonic energy transmitted from the stringer to the frame is sufficient for the detection of cracks in the frame. This modelling will provide useful information on the optimal placement of actuators and sensors for crack detection in realistic aircraft structures.

2.2 Finite Element Model (FEM)

The finite element analysis software used for this investigation (NE Nastran) has been validated for the study of the propagating stress waves in plate-like structures by Koh et al [7], Rosalie et al [9] and Wong et al [10]. This work builds on the expertise developed for a built-up fuselage structure.

Acousto-ultrasonics involves the use of high frequency waves (in the order to 200 KHz). The size of the elements must be sufficiently small to accommodate the spatial characteristics of the propagating waves. The time-steps must also be adjusted to accordingly model the temporal characteristics of the propagating waves. This results in a large number of elements in the model and large computational times. The output files can also be large to capture the essential features of the waves.

In this work, a typical fuselage shell panel of 520mm × 180mm with the intersection of a stringer and a frame was modelled (Figure 2). The skin panel was assumed to be flat (i.e. without any curvature). The cross sections of the stringer and the frame were assumed to be the same along their length. The overall dimension of the panel and a front view are shown in Figures 2 and 3. The areas within the dark line in Figure 2 are where the clip was contacted to the skin, the stringer and the frame. The connections between the clip and the skin, the stringer and the frame were fastened by rivets. The locations of the rivets on the clips are shown in 4.

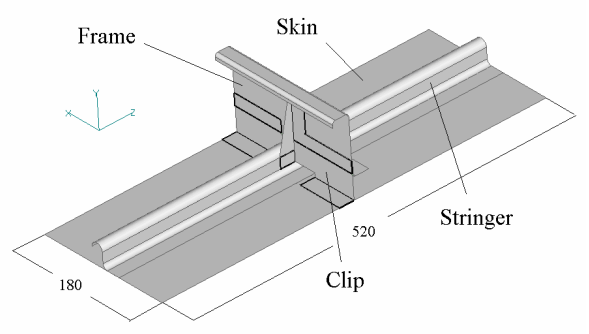

Fig. 2. Fuselage shell model (units mm)

As the length of the skin, the stringer and the frame are relatively large compared to their

thickness, a two-dimensional finite element model was used in this work.

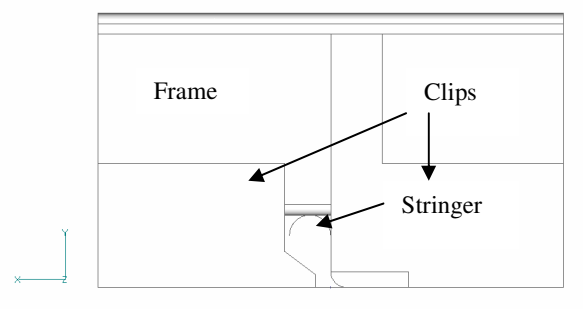

Fig. 3. Front view of fuselage model

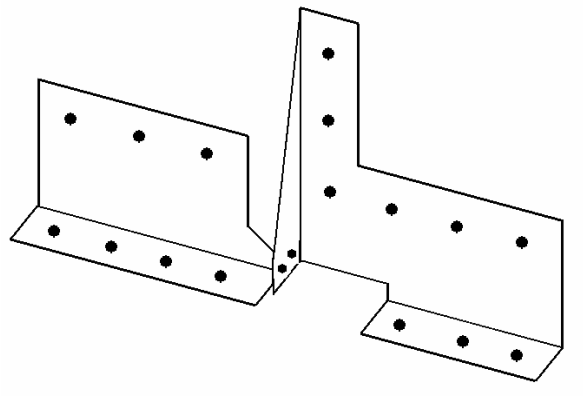

Fig. 4. Illustration of the clips

2.3 Material Properties and Input Stress Pulse

The materials used in the model are 2024 aluminium, in different tempers for skin (T3), stringer (T351) and frame (T42). The details of the most important mechanical properties of the aluminium alloys used for the analysis are given in Table 1.

Table 1. Material properties

Materials	skin	stringer	frame	clip
Young's modulus E (GPa)	72.4	74.5	77.0	72.4
Density ρ (g/cm^3)	2.80	2.77	2.66	2.80
Thickness t (mm)	2.5	2.0	1.6	1.0

A high frequency stress wave was assumed to be excited by the PZT and this is modelled via the application of an input pulse perpendicular to the surface of the structure. Figure 5 shows such an input stress pulse with duration of 0.5μs and its amplitude of 0.1MPa. The input pulse has a bandwidth of 2 MHz.

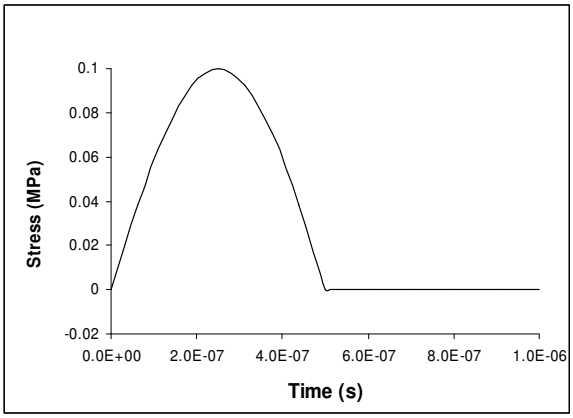

Fig. 5. Input stress pulse

2.4 Locations of the Cracks and Sensors

The aim of this work is to establish if acousto-ultrasonic waves can be used to detect the presence of cracks in a typical fuselage structure. For the purpose of this investigation, the crack is assumed to have developed across the entire stringer or the frame. The following cases were analysed.

Case 1: Both actuating and sensing PZTs located on the stringer

In this part of the analysis, a crack is assumed to have developed across the entire stringer. Figure 6 shows the 3 different crack locations analysed. An actuating PZT was located at Position A along the stringer. Cracks were located at positions identified as "crack1", "crack2" and "crack3". A sensing PZT is assumed to be located at Position B. The stress waves generated by the actuating PZT are propagated along the stringer and are detected by the sensing PZT at location B. The effect of cracks at the locations "crack1", "crack2" and "crack3" on the propagating stress wave was investigated.

In addition, the effect of cracks located on the frame (i.e. "crack4" and "crack5") on the propagating stress wave generated by the actuating PZT located at Position A and sensed at Position B (both on the stringer), was also investigated (Figure 7). This analysis was

performed to determine the effect of remote cracks on the propagating stress wave along the stringer.

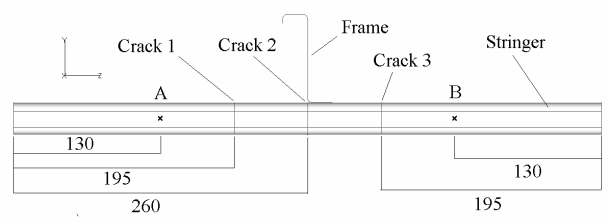

Fig. 6. Crack and PZT location on stringer (mm)

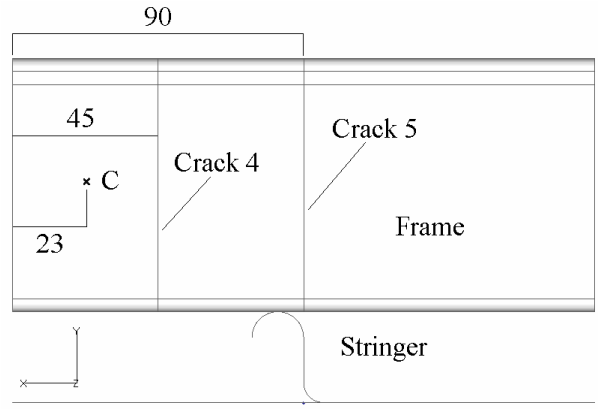

Fig. 7. Crack and PZT location on frame (mm)

Case 2: Actuating PZT and sensing PZT located on stringer and frame respectively.

In this analysis, the sensing PZT is located at Position C on the frame. The actuating PZT is located at Point A along the stringer. The effect of cracks existing at locations "crack1" and "crack4" on the stress wave generated at Position A and sensed at Position C was investigated.

In both cases described above, a separate set of analyses were performed with no cracks on both the stringer and the frame (i.e "Healthy structure"). The solution to these "no crack" cases were used as a baseline solution. It is envisaged that the results from Case 1 and Case 2 will have implications in the location of PZTs in the fuselage section for crack detection.

2.5 Experimental Trials

A set of Al test components matching the fuselage shell model were manufactured to allow the following specific cases to be experimentally measured.

a) Uncracked "healthy" structure with PZT actuator at position A and PZT sensors at positions B (Case 1) and C (Case 2).

b) PZT actuator at A, PZT sensor at B and "crack1" present (Case 1).

c) PZT actuator at A, PZT sensor at B and "crack2" present (Case 1).

d) PZT actuator at A, PZT sensor at B and "crack5" present (Case 1).

e) PZT actuator at A, PZT sensor at C and "crack1" present (Case 2).

The results of these tests were then compared to the outputs of the NE Nastran analysis to verify the accuracy of the modelling.

3 Results and Discussion

3.1 Case 1: Both Actuators and Sensors on the Stringer

As discussed in the above section, an actuator used to excite an ultrasonic wave into the structure was located at the Position A on the stringer (see Figure 6). The sensing PZT is located at Position B of the stringer. The results are shown in Figure 8 to Figure 10. Figure 8 shows the response for all cases analysed. The responses of three cracks located in the stringer are shown in Figure 9 and the responses of two cracks in the frame are compared with healthy structure in Figure 10.

Figure 8 shows the results obtained from all crack locations. These results are best analysed with Figure 9 and Figure 10. Figure 9 shows the response obtained where the cracks were located along the stringer. Whilst the solution appears to be unaffected by the location of the crack, it is significantly lower than the solution obtained from the "healthy structure". Therefore cracks within the stringer can be identified by a PZT actuator/sensor pair although their precise location is difficult to determine.

Figure 10 shows the results obtained with the cracks along the frame. The results show

that the stress wave propagating along the stringer is unaffected by the presence of the cracks in the frame. Therefore cracks in the frame cannot be identified by a PZT actuator/sensor pair on the stringer.

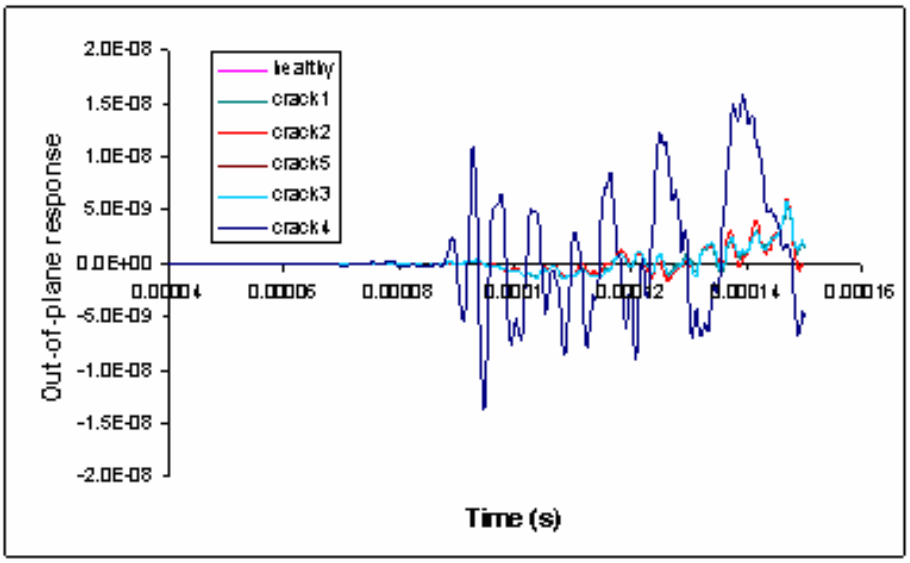

Fig. 8. Out of plane response for all crack locations

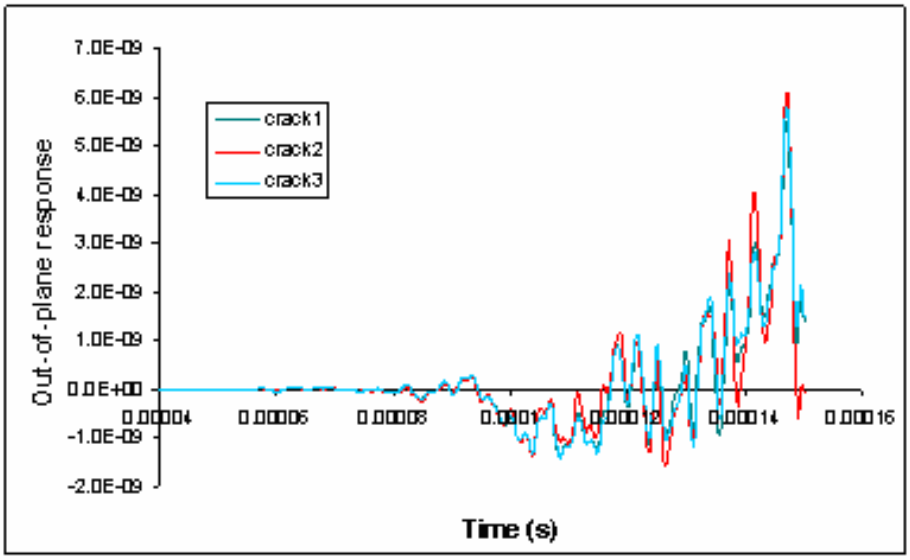

Fig. 9. Out of plane response for stringer cracks

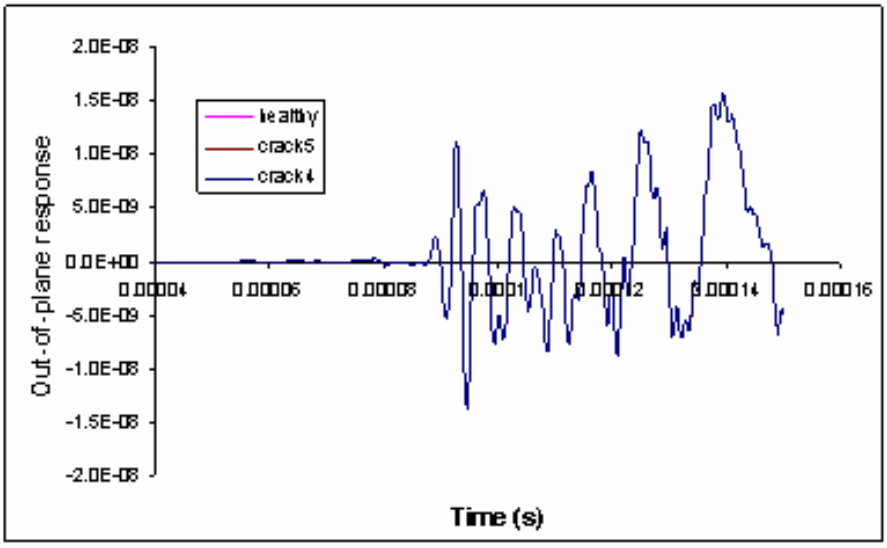

Fig. 10. Out of plane response for cracks in frame

Figure 11 shows the comparison between the experimental tests and the FE analysis. The Root Mean Square (RMS) of the signal received by the PZT sensor was used to indicate the strength of the signal in the various specimens. The response was also normalised with respect to the response from the undamaged specimen so that the relative decrease in signal strength could be illustrated for each situation.

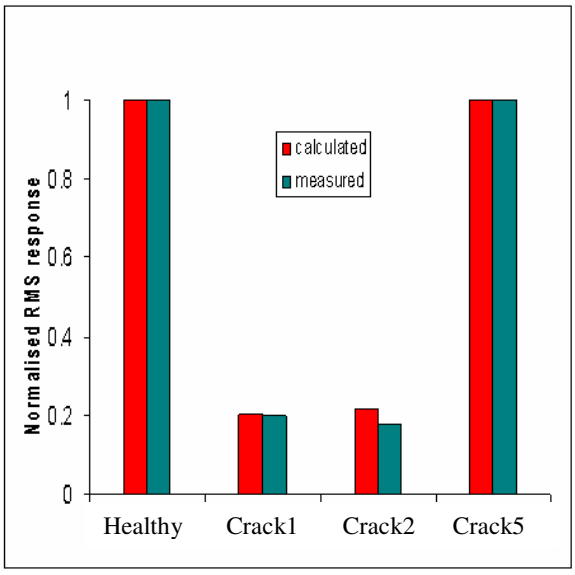

Fig. 11. Comparison of predicted and experimental results for Case 1

The comparison between the predicted and experimental response is very good, suggesting that the NE Nastran analysis is modelling the acousto-ultrasonic response of the Al component accurately.

3.2 Case 2: Actuator on the Stringer and Sensor on the Frame

In this part of the investigation, the actuator was located at "Position A" on the stringer while the sensor is now located on "Position C" on the frame (Figure 7). The three set of analyses performed were:

(a) a healthy structure
(b) crack on the stringer (crack1)
(c) crack on the frame (crack4).

Figure 12 shows the results obtained from these analyses. The responses obtained from the damaged structures were compared with that obtained from the healthy structure. The following observations were made from these analyses:

By locating the sensing point on the frame, a stress wave generated on the stiffener is sensitive to the presence of the crack on the stringer and also on the frame. In both cases the crack on the stringer and the crack on the frame are in the path of propagating stress wave

between the actuating point (Position A) and sensing point (Position C).

The feasibility of using an actuator located on a stringer and a sensor located on the frame configuration can be assessed by the relative strength of the signal obtained when both the actuating and the sensing PZTs were located along the stringer. Figure 13 shows the comparison of the magnitude of the response obtained with a sensor located on the frame with that where the sensor was located on the stringer. The response of the healthy structure received from the sensor located on the frame is smaller than that received from the stringer of the cracked structure. The apparent difference in the energy transmitted may be a limiting factor for the use of a sensor located on the frame to detect stress waves actuated on the stringer.

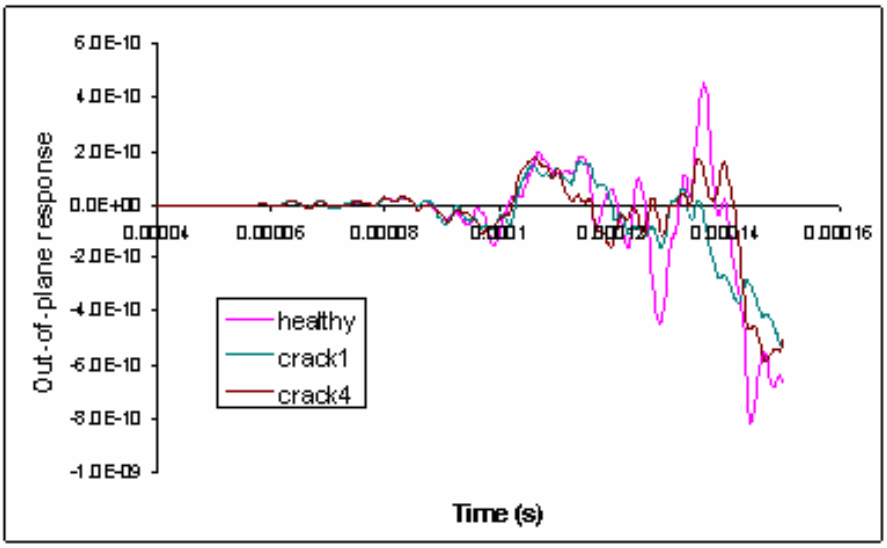

Fig. 12. Out of plane response for Case 2

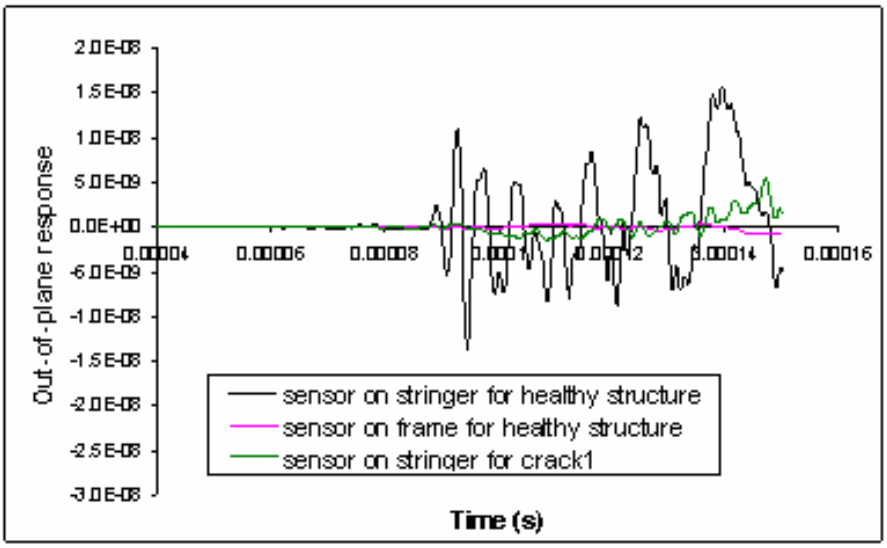

Fig. 13. Comparison of signal response for sensors on stringer and frame

Figure 14 shows the comparison between the experimental tests and the FE analysis. As before, the normalized Root Mean Square (RMS) of the signal received by the PZT sensor was used to indicate the strength of the response in the various specimens.

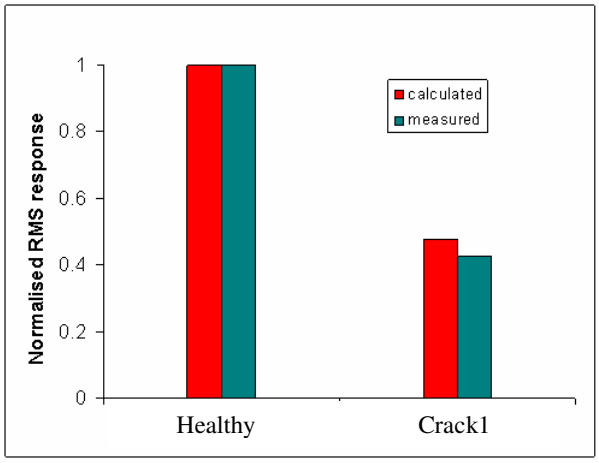

Fig. 14. Comparison of predicted and experimental results for Case 2

Again the comparison between the predicted and experimental response is very good, suggesting that the NE Nastran analysis is modelling the acousto-ultrasonic response of the Al component accurately.

4 Conclusions

The following conclusions can be drawn from the work presented in this paper:

The FEM investigation presented in this paper demonstrates the feasibility of acousto-ultrasonic stress waves produced by PZT actuators being used for identifying cracks in a typical Al fuselage structure.

A pair of PZT actuators/sensors located on the stringer is able to detect the presence of cracks between them. However, for cracks outside the stringer (e.g. cracks along the frame) no effect on the propagating stress waves can be determined. Therefore actuator/sensors pairs on one structural feature are unlikely to identify damage on a neighbouring feature.

The stress waves generated by an actuator located on the stringer can also be used to detect cracks on the frame when a sensor is placed upon the frame. This is only possible if the crack is located along the propagating direction of the stress wave. However, the signal intensity recorded by the sensor on the frame is very low in comparison to the case where the sensor is located on the stringer.

These results suggest that it may therefore be possible to create an optimal network of actuators and sensors so that both stringers and frames are monitored without the need to use excessive numbers of devices.

References

[1] Chimenti D and Martin R. Nondestructive evaluation of composite laminates by leaky lamb waves. *Ultrasonics*, Vol. 29, pp. 13–21, 1991.

[2] Cheng J and Berthelot Y. Theory of laser-generated transient lamb waves in orthotropic plates. *Journal of Physics D: Applied Physics*, Vol. 29, pp. 1857–1867, 1996.

[3] Bork U and Challis R. Non-destructive evaluation of the adhesive fillet size in a T-peel joint using ultrasonic lamb waves and a linear network for data discrimination. *Measurement Science and Technology*, Vol. 6, pp. 72–84, 1995.

[4] Rokhlin S. Lamb wave interaction with lap-shear adhesive joints: theory and experiment. *J Acoust Soc Am,* Vol. 89, pp 2758–2765, 1991.

[5] Todd C and Challis R. Quantitative classification of adhesive bondline dimensions using lamb waves and artificial neural networks. *IEEE Transactions on Ultrasonics, Ferroelectrics and Frequency Control* Vol. 46, No. 1, pp. 167–181, 1999.

[6] Rokhlin S and Bendec F. Coupling of lamb waves with the aperture between two elastic sheets. *J Acoust Soc Am* Vol. 73, No. 1, pp 55–60, 1983.

[7] Rajic N, Galea S and Chiu W. Autonomous Detection of Crack Initiation Using Surface Mounted Piezotransducers. *Smart Materials and Structures*, Vol. 11, pp. 1-8, 2002.

[8] Koh Y, Chiu W and Rajic N. Integrity assessment of composite repair patch using propagating lamb wave. *Composite Structures*, Vol. 58, pp 363-371, 2002.

[9] Koh Y, Chiu W and Rajic N. Effects of local stiffness changes and delamination on lamb wave transmission using surface-mounted piezoelectric transducers. *Composite Structures*, Vol. 57: pp 437-443, 2002.

[10] Wong C, Chiu W and Rajic N. Detection of disbands in scarf joints using lamb waves. *Proceedings of the 2nd Australasian Workshop on Structural Health Monitoring*, Melbourne, Australia, paper 21, 2004